Journal of Atmospheric and Solar-Terrestrial Physics 121 (2014) 24–31

Contents lists available at ScienceDirect

Journal of Atmospheric and Solar-Terrestrial Physics

journal homepage: www.elsevier.com/locate/jastp

Superposed epoch analyses of HILDCAAs and their interplanetary drivers: Solar cycle and seasonal dependences

Rajkumar Hajra [a,*], Ezequiel Echer [a], Bruce T. Tsurutani [b], Walter D. Gonzalez [a]

[a] Instituto Nacional de Pesquisas Espaciais (INPE), Av. dos Astronautas, 1758, Sao Jose dos Campos, SP 12227-010, Brazil
[b] Jet Propulsion Laboratory, California Institute of Technology, 4800 Oak Grove Drive Pasadena, California 91109, Pasadena, CA, USA

ARTICLE INFO

Article history:
Received 28 March 2014
Received in revised form
19 September 2014
Accepted 23 September 2014

Keywords:
HILDCAAs
High-speed streams
CIRs
Solar cycle phases

ABSTRACT

We study the solar cycle and seasonal dependences of high-intensity, long-duration, continuous AE activity (HILDCAA) events and associated solar wind/interplanetary external drivers for ~$3\frac{1}{2}$ solar cycle period, from 1975 to 2011. 99 HILDCAAs which had simultaneous solar wind/interplanetary data are considered in the present analyses. The peak occurrence frequency of HILDCAAs was found to be in the descending phase of the solar cycle. These events had the strongest time-integrated AE intensities and were coincident with peak occurrences of high-speed solar wind streams. The event initiations were statistically coincident with high-to-slow speed stream interactions, compressions in the solar wind plasma and interplanetary magnetic field (IMF). The latter were corotating interaction regions (CIRs). The signatures of related CIRs were most prominent for the events occurring during the descending and solar minimum phases of the solar cycles. For these events, the solar wind speed increased by ~41% and ~57% across the CIRs, respectively. There was weak or no stream–stream interaction or CIR structure during the ascending and solar maximum phases. HILDCAAs occurring during spring and fall seasons were found to occur preferentially in negative and positive IMF sector regions (toward and away from the Sun), respectively.

1. Introduction

High-intensity, long-duration, continuous AE activity (HILDCAA) events are known to be associated mostly with high-speed solar wind streams (HSSs) (Tsurutani and Gonzalez, 1987; Tsurutani et al., 1995, 2006a; Hajra et al., 2013, 2014a,b). These geoeffective events are distinguished from other types of geomagnetic activity by four strict criteria, as proposed by Tsurutani and Gonzalez (1987): (i) HILDCAAs are defined to be intervals of intense auroral activities characterized by peak AE intensities greater than 1000 nT, (ii) have a minimum of 2 days duration, when (iii) AE values do not drop below 200 nT for more than 2 h at a time. These events are also defined (iv) to occur outside of the main phases of the geomagnetic storms. In general, HILDCAAs are found to be associated with weak ring current enhancements ($Dst \geq -50$ nT), recovery phases of geomagnetic storms, or independent of storms. The study of Tsurutani and Gonzalez (1987) reported a one-to-one correspondence of HILDCAAs with interplanetary Alfvén waves (Belcher and Davis, 1971) accompanying the HSSs (Tsurutani et al., 2005, 2006a,b). The auroral activity is attributed to the solar wind energy transfer into the magnetosphere by the continuous, sporadic magnetic reconnection between Earth's magnetopause field and southward component of the interplanetary Alfvén waves (Tsurutani and Gonzalez, 1987; Tsurutani et al., 1995; Hajra et al., 2014a).

A recent study by Hajra et al. (2013) found that HILDCAA events statistically start in the positive gradients of solar wind speed (Vsw) and plasma temperature (Tsw). These were found to be associated with typical signatures of corotating interaction regions (CIRs), high-to-slow speed stream interactions causing solar wind plasma and magnetic field compressions (Smith and Wolfe, 1976; Tsurutani et al., 2006a). The HILDCAA intervals were shown to be well-correlated with the HSS events. On the other hand, there was a small number (6%) of events related to interplanetary coronal mass ejections (ICMEs).

It has been shown (Hajra et al., 2014b) that HILDCAA events are associated with generation of magnetospheric relativistic electron acceleration (Paulikas and Blake, 1979; Baker et al., 1986; Summers et al., 1998; Meredith et al., 2003; Tsurutani et al., 2006a,b; Hajra et al., 2013). The relativistic electrons are known as "killer electrons" for their hazardous effects to orbiting spacecraft (Wrenn, 1995; Horne, 2003). Also, a majority of the solar wind energy input is shown to be dissipated in the outer magnetosphere and ionosphere during HILDCAA events (e.g., Hajra et al., 2014a).

* Corresponding author.
E-mail address: rajkumarhajra@yahoo.co.in (R. Hajra).

http://dx.doi.org/10.1016/j.jastp.2014.09.012
1364-6826/

These make HILDCAA events important aspects of modern space weather studies. The aim of the present study is to investigate the general geomagnetic characteristics of HILDCAAs and associated interplanetary structures. The method of superposed epoch analysis is applied to the events occurring during ~$3\frac{1}{2}$ solar cycles (1975–2011). Although each event has its own distinctive characteristics, we apply a statistical approach in order to identify common elements and patterns. The ultimate goal is to understand the basic physical mechanisms for the HILDCAA events. We also investigate possible solar cycle and seasonal dependences. Although magnetic storms and their solar/interplanetary drivers have been investigated for almost 50 years (e.g., Rostoker and Falthammar, 1967; Gonzalez and Tsurutani, 1987; Gonzalez et al., 1994; Gosling et al., 1990; Huttunen and Koskinen, 2004; Echer et al., 2008; Hutchinson et al., 2011, and references therein), there has been no such study on the solar/interplanetary drivers of HILDCAAs using statistical means to date.

2. Data and method of analysis

As indicated in Section 1, HILDCAA events were identified by four criteria (Tsurutani and Gonzalez, 1987):

(i) the events had peak AE intensities greater than 1000 nT,
(ii) the events had durations at least 2 days in length,
(iii) the high AE activity was continuous throughout the interval, i.e., AE never dropped below 200 nT for more than 2 h at a time, and
(iv) the events occurred outside the main phases of geomagnetic storms.

To identify HILDCAA events, we first detected intervals with AE > 1000 nT. The data were scanned both forward and backward in time to determine where the event decreased below 200 nT for 2 h or more. If this interval was outside of a storm main phase (Dst < −50 nT: Akasofu, 1981; Gonzalez et al., 1994) and was longer than 2 days, this was categorized as a HILDCAA event. Using this methodology, Hajra et al. (2013) developed a list of 133 HILDCAA events occurring during ~$3\frac{1}{2}$ solar cycle period, from 1975 through 2011. The list of the events is available, upon request, for studies of chorus, relativistic electrons, as well as ionospheric and geomagnetic effects. Of the 133 events, 99 had simultaneous geomagnetic and solar wind/interplanetary data available. We study the latter events here. The geomagnetic data (1 h resolution) were obtained from the World Data Centre for Geomagnetism, Kyoto, Japan (http://wdc.kugi.kyoto-u.ac.jp/). The solar wind data (1 min resolution) were obtained from the OMNI website (http://omniweb.gsfc.nasa.gov/). The latter data had been already time-shifted to coincide with solar wind convective times of impingement at the nose of the magnetopause.

To study the solar cycle dependences, the events were separated into four solar cycle phases: the ascending (1977–1978, 1987–1988, 1998–1999, 2011), solar maximum (1979–1981, 1989–1991, 2000–2002), the descending (1982–1984, 1992–1994, 2003–2005), and solar minimum (1975–1976, 1985–1986, 1995–1997, 2006–2010) phases. Annual averaged $F_{10.7}$ solar flux (10^{-22} W m^{-2} Hz^{-1}) data (http://www.drao.nrc.ca/icarus) were used to identify solar cycle phases. The events were also grouped into four (northern hemispheric) seasons defined as follows: spring equinox (February, March, April), summer solstice (May, June, July), fall equinox (August, September, October), and winter solstice (November, December, January).

3. Results

3.1. Solar cycle dependences

In the upper panel of Fig. 1 the histogram shows the occurrence frequency of HILDCAAs (N^{y}_{H}) over the interval of study (1975–2011). This is the number of events in a year divided by the number of months when observations were available for that particular year. AE gaps are denoted by a "G". Also shown in the

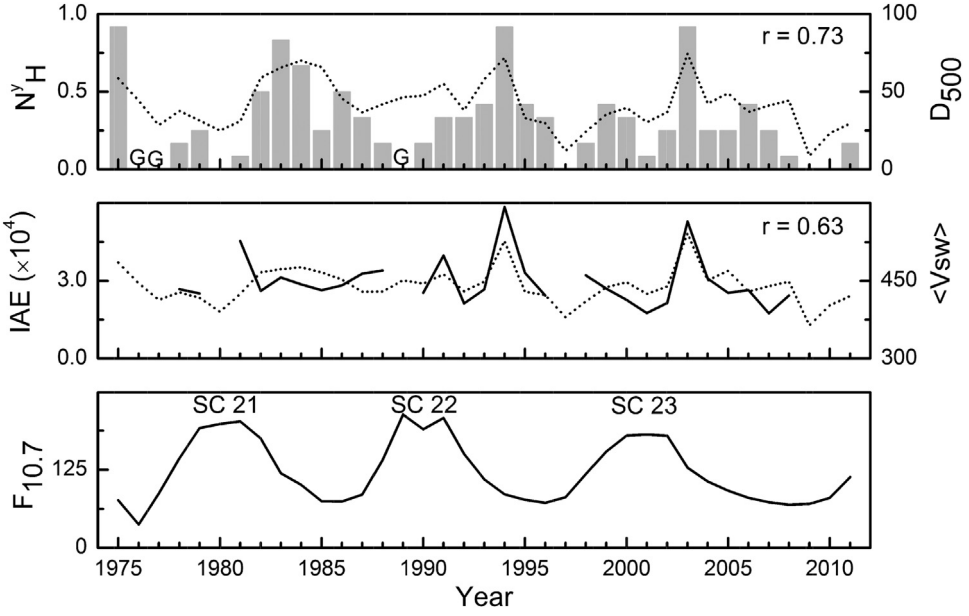

Fig. 1. Histogram (legend on the left) in the top panel gives the yearly HILDCAA numbers (N^{y}_{H}) normalized by months of observation. The "G"s represent AE data gaps from January 1976 to December 1977, from July 1988 to February 1989, and from April to December of 1989. The dotted curve (legend on the right) in the same panel shows the yearly mean values of percentage occurrence of HSSs (D_{500} in percentage). In the middle panel, the solid line (legend on the left) shows the time-integrated AE strength (IAE in nT h). The dotted curve (legend on the right) in the middle panel shows the yearly mean solar wind speed (⟨Vsw⟩ in km/s). The linear regression coefficients (r) between N^{y}_{H} and D_{500}, and between IAE and ⟨Vsw⟩ are indicated in the upper right of each panel. Both correlations are statistically significant at a > 95% confidence level. The bottom panel shows the variation of yearly mean $F_{10.7}$ solar flux for the entire period of observation. Solar cycles (SCs) are marked in the bottom panel.

same panel is the yearly percentage occurrence (D_{500}) of HSSs (peak solar wind speed Vsw $\geq$ 500 km/s: see Hirshberg, 1975; Broussard et al., 1977; Xanthakis et al., 1988). In the middle panel, the solid and dotted lines show the yearly mean values of time-integrated AE intensity (IAE in nT h) of HILDCAAs and the yearly mean solar wind speed ($\langle$Vsw$\rangle$ in km/s), respectively. IAE refers to AE index integrated over the HILDCAA event. Discontinuities in IAE are due to absence of any HILDCAA (1997, 2009, 2010). It may be mentioned that we considered the integrated strength (IAE) to characterize the HILDCAAs as these are known to be intervals when high AE activity continues for days. The bottom panel shows the variation of yearly mean $F_{10.7}$ solar fluxes which are used to identify solar cycle phases, described in Section 2.

As reported previously (Hajra et al., 2013), HILDCAAs occur preferentially during the descending phase of the solar cycles, and they exhibit strong association with HSSs. N_H^Y exhibited statistically significant correlation with D_{500} (linear regression coefficient, r=0.73) and $\langle$Vsw$\rangle$ (r=0.79). We note here that IAE also followed the variation of $\langle$Vsw$\rangle$. While the coefficient of liner regression between the two parameters is low (r=0.63) for the entire period of observation, the coincidences of peaks in IAE during 1994 and 2003 with those of $\langle$Vsw$\rangle$ are remarkable. Solar wind is dominated by HSSs during these two years in the declining phase of the solar cycles 22 and 23, respectively (e.g., Tsurutani et al., 2011a). It is interesting to note that descending phase of solar cycle 21 is quite different in the variations of D_{500}, $\langle$Vsw$\rangle$ and IAE compared to the other solar cycles. Both the IAE and $\langle$Vsw$\rangle$ curves are relatively flat with no clear one year peak. Further study may be done to understand the difference, which is out of the scope of the present study.

Superposed epoch analyses were performed on the solar wind/interplanetary and geomagnetic parameters: solar wind speed (Vsw in km/s), plasma density (Nsw in cm^{-3}), temperature (Tsw in K), IMF magnitude (Bo in nT), the Bx (nT), By (nT) and Bz (nT) components in geocentric solar magnetospheric (GSM) coordinate system, and the Dst (nT) and AE (nT) indices. The initiation time of the HILDCAA events was taken as the zero epoch time (see previous discussion). Fig. 2 shows the results of superposed analyses during four phases of the solar cycle. The hourly averages of the superposed values (solid curves) along with standard deviations (vertical bars) are shown in the figure. The standard deviations indicate that the ranges of variations of the parameters are very high. This seems to be typical for CIR/HSS events (see Liou, 2006; Lu, 2006; McPherron and Weygand, 2006; Liu et al., 2012). The average AE activity and Dst were somewhat more enhanced during the ascending phase (AE$\sim$513 nT, Dst~ -35 nT) and solar maximum ($\sim$606 nT, -46 nT) in comparison to the descending phase ($\sim$502 nT, -32 nT) and to solar minimum ($\sim$484 nT, -32 nT). During the ascending phase and solar maximum, the pre-event AE and Dst values were also enhanced. The average durations of the events in the descending phase ($\sim$3.3 days) and solar minimum ($\sim$3.5 days) were comparatively longer than in the ascending phase ($\sim$2.7 days) and solar maximum ($\sim$2.7 days). These resulted in higher IAE during the descending and solar minimum phases as revealed in Fig. 1.

The fast stream–slow stream interaction (in Vsw) was more pronounced during the descending and solar minimum phases than during the ascending and solar maximum phases. If we consider one day before the zero epoch time to one day after it, the slow-to-high speed increases were $\sim$41% and $\sim$57% for the

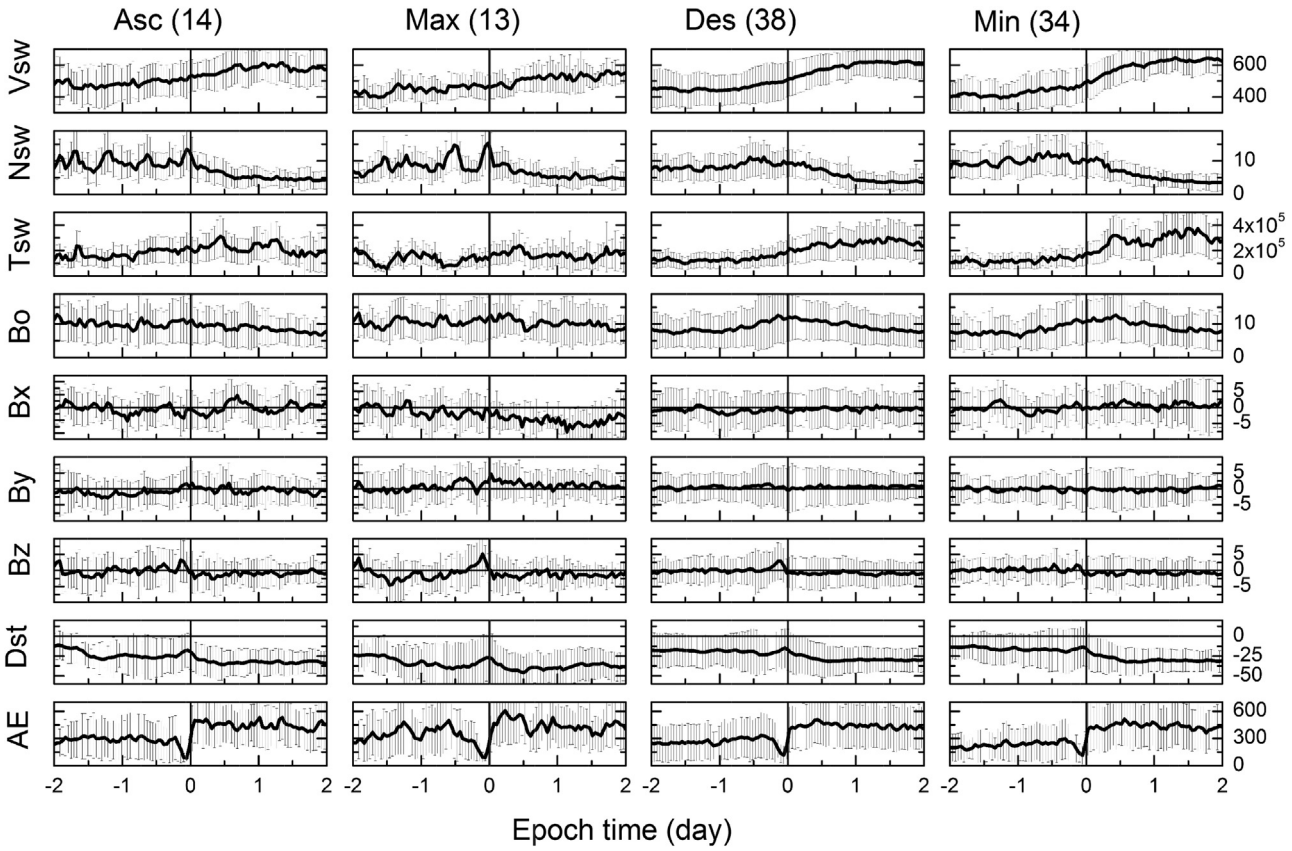

Fig. 2. Superposed epoch analyses results showing, from top to bottom panels, solar wind speed (Vsw in km/s), plasma density (Nsw in cm^{-3}), temperature (Tsw in K), IMF magnitude (Bo in nT), the Bx (nT), By (nT), Bz (nT) components in the GSM coordinate system, and the Dst (nT) and AE (nT) indices, respectively. The curves show the average values while the vertical bars show the standard deviations. The panels from left to right pertain to events occurring during four phases of the solar cycle: the ascending phase (Asc), solar maximum (Max), the descending phase (Des) and solar minimum (Min). The numbers in the bracket in the title indicate the total number of the events for the superposed analyses. The zero epoch time corresponds to the initiation times of HILDCAAs.

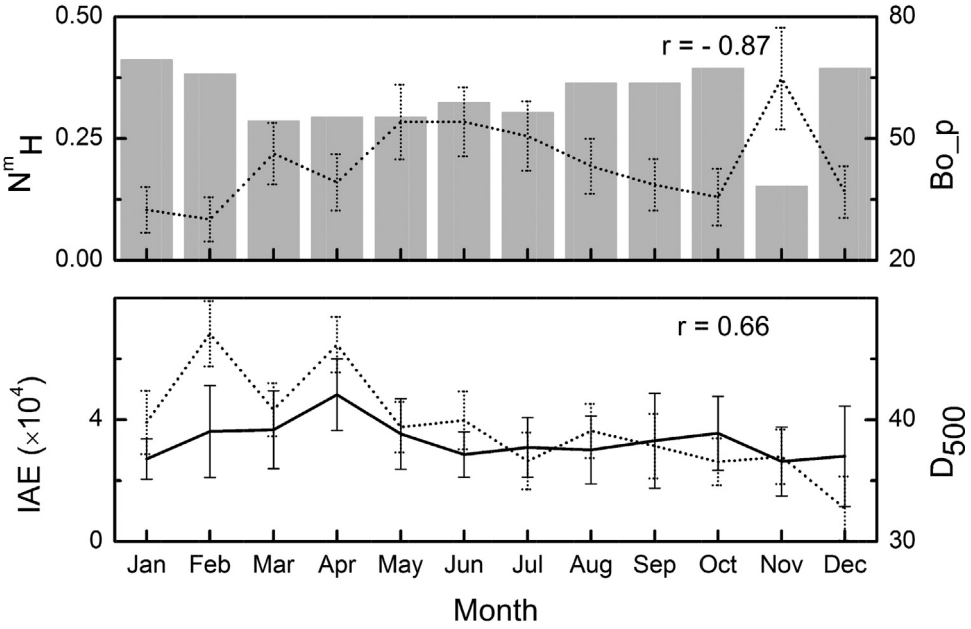

Fig. 3. Histogram (legend on the left) in the top panel shows monthly superposed distributions of HILDCAA events (N^m_H) normalized by years of observation. The dotted line (legend on the right) in the same panel shows the monthly mean values of peak IMF magnitude (Bo_p in nT). In the bottom panel, the continuous (legend on the left) and the dotted (legend on the right) curves show the monthly mean values of the time-integrated AE strength (IAE in nT h) and the percentage of days with HSSs (D_{500} in percentage) respectively. The standard deviations of Bo_p and D_{500} are shown by vertical dotted bars, while solid bars show standard deviations of IAE. The linear regression coefficients (r) between N^m_H and Bo_p, and between IAE and D_{500} are given in the upper right of each panel. Both the coefficients are statistically significant at a $>95\%$ confidence level.

descending and solar minimum phases, respectively. The average speeds around the peaks were about ~620 km/s and ~640 km/s, respectively, for these two phases. No such feature was observed during the ascending phase or solar maximum years and the average solar wind speeds (~580 km/s and ~550 km/s, respectively) were comparatively lower during HILDCAA intervals for these events. Superposed IMF Bz exhibited northward-to-southward turning prior to the initiation of the event under all solar activity conditions. It may represent the typical heliospheric current sheet (HCS) crossing occurring prior to stream interaction (Smith et al., 1978; Tsurutani et al., 1995). The superposed Bz showed larger and longer-duration southward excursions during solar maximum and the ascending phases than during the descending and minimum phase conditions. This is consistent with comparatively enhanced level of AE activity and Dst during the ascending and solar maximum phases due to enhanced solar wind-magnetospheric energy coupling.

3.2. Seasonal dependences

Fig. 3 shows variations of monthly mean occurrence frequency (N^m_H) and time-integrated AE intensity (IAE) of HILDCAAs during the entire interval of observations (1975–2011). N^m_H gives the number of events in a month divided by the number of years when observations were available for that particular month. The monthly averages (dotted lines) of peak IMF amplitude (Bo_p) and percentage occurrence (D_{500}) of HSSs are also superposed in the two panels for comparison. The vertical dotted bars show the standard deviations of Bo_p and D_{500}. The solid vertical bars show standard deviations of IAE. The IAE was found to follow the seasonal variation of D_{500} (correlation coefficient, $r=0.66$). The spring equinox (April) events were ~67% stronger (IAE) than the events occurring during other seasons. There was not much difference in IAE between fall and the solstices. The seasonal distribution of N^m_H was much more ambiguous, the only prominent feature was minimum occurrence during November. Interestingly, the same period was characterized by strong annual peak in IMF Bo. N^m_H exhibited strong anti-correlation with Bo_p ($r=-0.87$). This figure shows seasonal pattern of HILDCAA parameters averaged over more than three solar cycles (1975–2011). Clearly, HILDCAA occurrence frequency or HILDCAA strength did not exhibit any "classical" semiannual variation such as those reported for other forms of geomagnetic activity (Sabine, 1852; Cortie, 1912; Priester and Catanni, 1962; Chakraborty and Hajra, 2010; Echer et al., 2011; Hajra, 2011).

Fig. 4 shows superposed interplanetary and geomagnetic parameters for HILDCAA events occurring during the spring, summer, fall and winter seasons. There seems to be no obvious seasonal features of geomagnetic activity associated with HILDCAAs. Only minor seasonal effects were found. The average AE activity seemed to be weakest for winter-events (~412 nT) compared to summer (~523 nT), spring (~515 nT) and fall (~512 nT) events, while Dst values were found to be more enhanced during the equinoxes (~−42 nT for spring, ~−35 nT for fall) in comparison to the solstices (~−25 nT for summer, ~−27 nT for winter).

The magnetic field (Bo) compression (>40%) was most prominent during the solstices, while little or no signatures of field compressions were noted during fall. The variations of Vsw gave the standard signatures of stream–stream interactions more-or-less for all seasons, although the slow-to-fast speed increases seemed to be slightly larger during the solstices (~38% for summer, ~42% for winter) than for the equinoxes (~30% for spring, ~27% for fall). However, the events during different seasons seem to be associated with more-or-less the same interplanetary structures (CIRs).

The variations of IMF Bx and By components were examined during the equinoxes. During the spring equinox, the average Bx was positive and By was negative well before the statistical event initiation and during the HILDCAA interval, indicating negative (towards the Sun) IMF sector region. Positive (away from the Sun) IMF sector region was prominent in the superposed variations of Bx (negative) and By (positive) during fall. We also checked the sector polarities of the solar wind as listed in the Wilcox Solar Observatory (http://wso.stanford.edu/). It is observed that 24

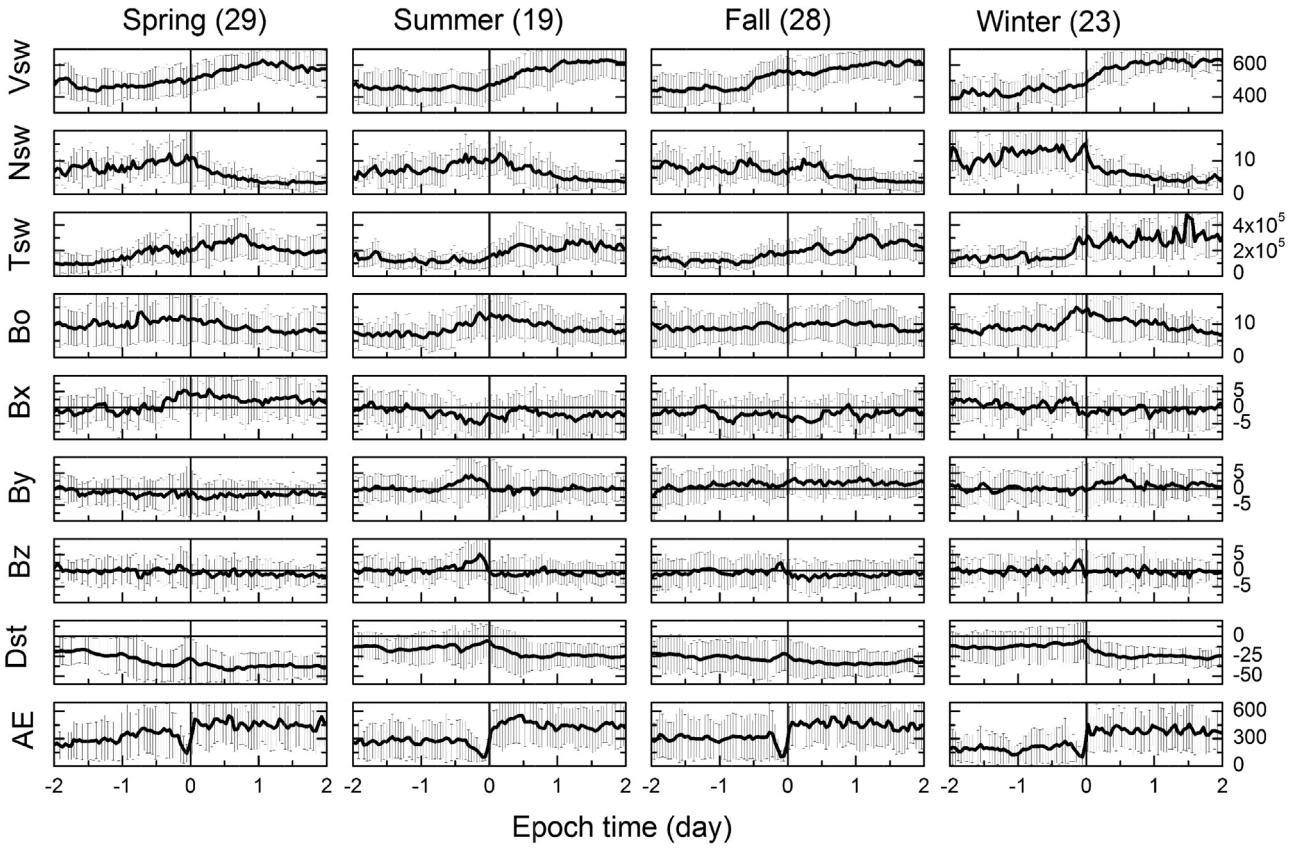

Fig. 4. The parameters in the panels from top to bottom are the same as in Fig. 2. From left to right, the panels show results for the four seasons (northern hemispheric): spring, summer, fall and winter. The numbers in the bracket in the title indicate the total number of the events for the superposed analyses.

HILDCAAs out of 29 occurring during spring and 24 out of 28 occurring during fall had these favorable IMF polarities (negative and positive during spring and fall, respectively).

4. Discussion

We studied the solar cycle and seasonal dependences of HILDCAAs and associated solar wind/interplanetary variations using the method of superposed epoch analysis. A total of 99 events occurring during 1975–2011 – a ~$3\frac{1}{2}$ solar cycle period – were considered.

Our earlier work (Hajra et al., 2013) showed that HILDCAAs, on average, correspond to a moderate level of geomagnetic activity (average AE ~500 nT, Dst > −50 nT). It may be mentioned that the averaged values (over a large number of events) are not hugely different from the ones for steady magnetospheric convection events. HILDCAA initiations coincided well with the fast stream–slow stream interactions in Vsw, while HILDCAA intervals were associated with HSS events. The magnetic field and plasma compressions were recorded in the variations of IMF Bo and Nsw, which are typical for CIRs preceding the HSS events (Smith and Wolfe, 1976). This sequence corroborated the schematic produced by Tsurutani et al. (1995, 2006a). While HILDCAA initiation was preceded by north-to-southward turning in IMF Bz, average Bz was generally negative during HILDCAA intervals. The present study continues this earlier work to investigate the solar cycle phase and seasonal effects.

HILDCAAs occurring during solar cycle maximum and the ascending phases were found to be different than those during solar cycle minimum and the descending phases both in character and causative solar wind/interplanetary variations. While the average ring current and auroral activity were comparatively more enhanced for solar maximum and the ascending phases, the average duration of the events was shorter than that during solar minimum and the descending phases. The events occurring during the descending phase of the solar cycles 22 and 23 had the largest integrated AE intensity, coincident with the peak occurrence of HSSs. The signatures of fast stream–slow stream interaction and compressions of solar plasma and magnetic field, i.e., CIR structures, were quite prominent for the events occurring during solar minimum and the descending phases. On the contrary, CIR structures were very weak or absent for the events during solar maximum and the ascending phases.

The above results are consistent with solar cycle variations of solar wind drivers of geomagnetic activity at the Earth. At and around the solar maximum, intense solar flares and coronal mass ejections (CMEs) or their interplanetary counterparts (ICMEs) are the main drivers of relatively intense geomagnetic activity (Burlaga et al., 1981; Gonzalez and Tsurutani, 1987; Gosling et al., 1990; Tsurutani and Gonzalez, 1997; Richardson et al., 2002; Echer et al., 2008). On the other hand, during the declining phase and solar minimum, HSSs emanating from equatorial/lower latitude solar coronal holes interact with slow background streams and form CIRs (Smith and Wolfe, 1976; Pizzo, 1985; Tsurutani et al., 1995; Balogh et al., 1999). The CIRs cause weak/moderate storms (Tsurutani and Gonzalez, 1987; Alves et al., 2006). The trailing HSS proper accompanied by Alfvén waves causes prolonged periods of geomagnetic activity (Tsurutani et al., 1995; Guarnieri et al., 2006; Kozyra et al., 2006; Turner et al., 2006). Although the HSS/HILDCAA intervals appear as “recovery phases” of CIR-storms, there is fresh input of solar wind energy (in addition to ring current decay) into the magnetosphere/magnetotail system (Tsurutani et al., 2004; Guarnieri, 2006; Hajra et al., 2014a).

When HILDCAAs were separated according to seasons and averaged over solar cycles, the spring equinox events exhibited ~67% stronger time-integrated AE intensity compared to events occurring during other seasons. The number of events was the smallest during November. Clearly, HILDCAAs did not exhibit any "classical" semiannual variation reported earlier for other forms of geomagnetic activity of varying intensity (Sabine, 1852; Cortie, 1912; Priester and Catanni, 1962). It may be noted that the above references showed the average variations over many years (more than one solar cycle) as we did in the present work (average over ~$3\frac{1}{2}$ solar cycles). This result may corroborate the findings of Mursula et al. (2011), suggesting ionospheric conductivity control on geomagnetic activity.

Monthly mean values of HILDCAA occurrence frequency exhibited anti-correlation with peak IMF amplitudes. The November events were the smallest in number and comparatively weaker in strength and shorter in duration compared to events during other seasons. The period was found to be associated with the annual peak in IMF amplitude. The IMF peak during November is consistent with the preferential occurrence of interplanetary shocks in November (Echer et al., 2005). As suggested by Echer et al., during the second half of the year, the shock formation/propagation is facilitated by lower solar wind bulk speeds and lower characteristic upstream wave speed (both Alfvénic and magnetosonic), compared to the yearly average values. This mechanism will cause compression of the magnetic fields and plasmas. With higher field strengths in general, random Bz fluctuations (with some southward components) will lead to greater geomagnetic activity. This is consistent with the scenario: more shocks, more ICMEs, less CIRs and less and weak HILDCAAs (in November).

HILDCAAs occurring in the four seasons were found to be associated with more-or-less the same interplanetary CIR structure. However, Vsw increases were slightly enhanced during solstices (~40%) than equinoxes (~30%). Liu et al. (2012), analyzing OMNI2 database during the years 1998–2010, found no seasonal preference in the occurrence of CIRs. Our results are consistent with those of Liu et al. Our present results are also consistent with the earlier results (Hajra et al., 2013) which noted a lack of any obvious seasonal dependence of HILDCAAs.

Another important result found is the preferential occurrence of spring and fall events in the negative (toward the Sun) and positive (away from the Sun) IMF sector regions, respectively. Equinoctial HILDCAAs occurred in "geoeffective" sector, where the IMF polarity had the greatest effect (McIntosh, 1959; Murayama, 1974; Berthelier, 1976; Clua de Gonzalez et al., 1993). The same result was suggested by Tsurutani et al. (2011b) based on the study of two HSS events during the declining phase of solar cycle 23. The IMF southward components are maximized during the "geoeffective" sector polarities and minimized during the "less geoeffective" sector polarities. It was shown that the main cause of geoeffectiveness of HSSs is the large-amplitude Alfvén waves while this seasonal effect may have a minor (~30%) contribution.

5. Conclusions

The main conclusions of the present study may be summarized as follows:

(1) The occurrence frequency and time-integrated AE intensities of HILDCAAs are highest during the descending phase of the solar cycle, coincident with the peak occurrences of high-speed solar wind streams.

(2) Superposed solar wind speeds (Vsw) exhibit ~41% and ~57% increases around the initiation times of HILDCAAs during the descending and solar minimum phases, respectively. This stream–steam interaction (CIR signature) is weaker or absent during the ascending and solar maximum phases.

(3) HILDCAAs occurring during different seasons were found to be associated with more or less the same interplanetary structures. However, Vsw increases were slightly enhanced during the solstices (~40%) than the equinoxes (~30%).

(4) HILDCAAs occurring during spring and fall were found to be associated with geoeffective negative (toward the Sun) and positive (away from the Sun) IMF sector regions, respectively.

(5) Although HILDCAAs exhibited no "classical" semiannual variations, the spring equinox events had ~67% stronger time-integrated AE intensity compared to events occurring during other seasons. The HILDCAA occurrence frequency was minimum during November. The latter period was associated with IMF peak due to preferential occurrence of interplanetary shocks as suggested by Echer et al. (2005).

6. Final comments

Some of the causes of the solar cycle effects can be understood by the position of the coronal hole relative to the HCS. During the declining phase, the current sheet has the nearly horizontal "ballerina skirt" shape (Smith et al., 1978). This places the coronal hole and HSS either above or below the HCS. Superradial expansion of the HSS will tend to push the HCS into the opposite hemisphere creating IMF Bz fields. In the other phase of the solar cycle, say during solar maximum, the HCS can be aligned nearly vertical to the ecliptic plane (Smith, 2001; Riley et al., 2002, and references therein). For this situation, superradial expansion of the HSS will push the HCS in an azimuthal direction with the creation of IMF By components, not Bz components.

The fact that many CIRs are present in the HILDCAA events and are influencing their superposed epoch analyses is an interesting one. The stream–stream interaction causing the compressed magnetic fields in the CIR with the amplified Alfvénic amplitudes is a natural process for producing high amplitude IMF Bsouth components and the initiation of HILDCAA events.

Acknowledgments

We wish to thank the two referees for their insightful and helpful comments. The work of R.H. is financially supported by Fundação de Amparo à Pesquisa do Estado de São Paulo (FAPESP) through post-doctoral research fellowship at INPE. E.E. would like to thank to the Brazilian CNPq (301233/2011-0) agency for financial support. Portions of this research were performed at the Jet Propulsion Laboratory, California Institute of Technology under contract with NASA.

References

Akasofu, S.-I., 1981. Relationships between the AE and Dst indices during geomagnetic storms. J. Geophys. Res. 86, 4820–4822. http://dx.doi.org/10.1029/JA086iA06p04820.

Alves, M.V., Echer, E., Gonzalez, W.D., 2006. Geoeffectiveness of corotating interaction regions as measured by Dst index. J. Geophys. Res. 111, A07S05http://dx.doi.org/10.1029/2005JA011379.

Baker, D.N., Blake, J.B., Klebesadel, R.W., Higbie, P.R., 1986. Highly relativistic electrons in the Earth's outer magnetosphere: 1. Life-times and temporal history 1979–1984. J. Geophys. Res. 91, 4265–4276. http://dx.doi.org/10.1029/JA091iA04p04265.

Balogh, A., Bothmer, V., Crooker, N.U., Forsyth, R.J., Gloeckler, G., Hewish, A., Hilchenbach, M., Kallenbach, R., Klecker, B., Linker, J.A., Lucek, E., Mann, G., Marsch, E., Posner, A., Richardson, I.G., Schmidt, J.M., Scholer, M., Wang, Y.M., Wimmer-Schweingruber, R.F., Aellig, M.R., Bochsler, P., Hefti, S., Mikic, Z., 1999. The solar origin of corotating interaction regions and their formation in the inner heliosphere. Space Sci. Rev. 89, 141–178.

Belcher, J.W., Davis, L., 1971. Large-amplitude Alfvén waves in the interplanetary medium: 2. J. Geophys. Res. 76, 3534–3563. http://dx.doi.org/10.1029/JA076i016p03534.

Berthelier, A., 1976. Influence of the polarity of the interplanetary magnetic field on the annual and the diurnal variations of magnetic activity. J. Geophys. Res. 81, 4546–4552.

Broussard, R.M., Sheeley, N.R., Tousey, R., Underwood, J.H., 1977. Stanford University Institute for Plasma Research. Report No. 696.

Burlaga, L.F., Sittler, E., Mariani, F., Schwenn, R., 1981. Magnetic loop behind and interplanetary shock: Voyager, Helios and IMP-8 observations.. J. Geophys. Res., 6; , pp. 6673–6684. http://dx.doi.org/10.1029/JA086iA08p06673.

Chakraborty, S.K., Hajra, R., 2010. Variability of total electron content near the crest of the equatorial anomaly during moderate geomagnetic storms. J. Atmos. Sol. Terr. Phys. 72, 900–911.

Clua de Gonzalez, A.L., Gonzalez, W.D., Dutra, S.L.G., Tsurutani, B.T., 1993. Periodic variation in the geomagnetic activity: a study based on the Ap index. J. Geophys. Res. 98, 9215–9231. http://dx.doi.org/10.1029/92JA02200.

Cortie, A.L., 1912. Sun-spots and terrestrial magnetic phenomena, 1898–1911. Mon. Not. R. Astron. Soc. 73, 52–60.

Echer, E., Gonzalez, W.D., Tsurutani, B.T., Vieira, L.E.A., Alves, M.V., Gonzalez, A.L.C., 2005. On the preferential occurrence of interplanetary shocks in July and November: causes (solar wind annual dependence) and consequences (intense magnetic storms). J. Geophys. Res. 110, A02101. http://dx.doi.org/10.1029/2004JA010527.

Echer, E., Gonzalez, W.D., Tsurutani, B.T., 2008. Interplanetary conditions leading to superintense geomagnetic storms (Dst ≤ -250 nT) during solar cycle 23. Geophys. Res. Lett. 35, L06S03http://dx.doi.org/10.1029/2007GL031755.

Echer, E., Tsurutani, B.T., Gonzalez, W.D., Kozyra, J.U., 2011. High speed stream properties and related geomagnetic activity during the whole heliosphere interval (WHI): 20 March to April 2008. Sol. Phys. , http://dx.doi.org/10.1007/s11207-011-9739-0.

Gonzalez, W.D., Tsurutani, B.T., 1987. Criteria of interplanetary parameters causing intense magnetic storms (Dst < -100 nT). Planet. Space Sci. 35, 1101–1109.

Gonzalez, W.D., Joselyn, J.A., Kamide, Y., Kroehl, H.W., Rostoker, G., Tsurutani, B.T., Vasyliunas, V., 1994. What is a geomagnetic storm? J. Geophys. Res. 99, 5771–5792.

Gosling, J.T., Bame, S.J., McComas, D.J., Phillips, J.L., 1990. Coronal mass ejections and large geomagnetic storms. Geophys. Res. Lett. 17, 901–904. http://dx.doi.org/10.1029/GL017i007p00901.

Guarnieri, F.L., 2006. The nature of auroras during high-intensity long-duration continuous AE activity (HILDCAA) events: 1998–2001. In: Tsurutani, B.T., McPherron, R.L., Gonzalez, W.D., Lu, G., Sobral, J.H.A., Gopalswamy, N. (Eds.), Recurrent Magnetic Storms: Corotating Solar Wind Streams. Geophysical Monograph Series, vol. 167. AGU, Washington, D.C., pp. 235–243.

Guarnieri, F.L., Tsurutani, B.T., Gonzalez, W.D., Echer, E., Gonzalez, A.L.C., Grande, M., Soraas, F., 2006. ICME and CIR Storms with Particular Emphasis on HILDCAA Events. ILWS Workshop 2006, Goa.

Hajra, R., 2011. A Study on the Variability of Total Electron Content Near the Crest of the Equatorial Anomaly in the Indian zone (Ph.D. thesis). University of Calcutta, India.

Hajra, R., Echer, E., Tsurutani, B.T., Gonzalez, W.D., 2013. Solar cycle dependence of high-intensity long-duration continuous AE activity (HILDCAA) events, relativistic electron predictors? J. Geophys. Res. 118, 5626–5638. http://dx.doi.org/10.1002/jgra.50530.

Hajra, R., Echer, E., Tsurutani, B.T., Gonzalez, W.D., 2014a. Solar wind-magnetosphere energy coupling efficiency and partitioning: HILDCAAs and preceding CIR storms during solar cycle 23. J. Geophys. Res. 119, http://dx.doi.org/10.1002/2013JA019646.

Hajra, R., Tsurutani, B.T., Echer, E., Gonzalez, W.D., 2014b. Relativistic electron acceleration during high-intensity, long-duration, continuous AE activity (HILDCAA) events: solar cycle phase dependences. Geophys. Res. Lett. 41, http://dx.doi.org/10.1002/2014GL059383.

Hirshberg, J., 1975. Composition of the solar wind: Present and past. Rev. Geophys. 13, 1059–1063. http://dx.doi.org/10.1029/RG013i003p01059.

Horne, R.B., 2003. Rationale and requirements for a European space weather programme, in: Proceedings of ESA Workshop, ESTEC, Noordwijk, The Netherlands.

Hutchinson, J.A., Wright, D.M., Milan, S.E., 2011. Geomagnetic storms over the last solar cycle: a superposed epoch analysis. J. Geophys. Res. 116, A09211. http://dx.doi.org/10.1029/2011JA016463.

Huttunen, K.E.J., Koskinen, H.E.J., 2004. Importance of post-shock streams and sheath region as drivers of intense magnetospheric storms and high-latitude activity. Ann. Geophys. 22, 1729–1738.

Kozyra, J.U., Criwley, G., Emery, B.A., Fang, X., Maris, G., Mlynczak, M.G., Niciejewski, R.J., Palo, S.E., Paxton, L.J., Randal, C.E., Rong, P.P., Russell, J.M.I.I.I., Skinner, W., Solomon, S.C., Talaat, E.R., Wu, Q., Yee, J.H., 2006. Response of the upper/middle atmosphere to coronal holes and powerful high-speed solar wind streams in 2003. In: Tsurutani, B.T., McPherron, R.L., Gonzalez, W.D., Lu, G., Sobral, J.H.A., Gopalswamy, N. (Eds.), Recurrent Magnetic Storms: Corotating Solar Wind Streams. Geophysical Monograph Series. AGU, Washington, D.C., pp. 319–340.

Liu, J., Liu, L., Zhao, B., Lei, J., Thayer, J.P., McPherron, R.L., 2012. Superposed epoch analyses of thermospheric response to CIRs: solar cycle and seasonal dependencies. J. Geophys. Res. 117, A00L10http://dx.doi.org/10.1029/2011JA017315.

Liou, K., 2006. Global auroral response to interplanetary media with emphasis on solar wind dynamic pressure enhancements. In: Tsurutani, B.T., McPherron, R.L., Gonzalez, W.D., Lu, G., Sobral, J.H.A., Gopalswamy, N. (Eds.), Recurrent Magnetic Storms: Corotating Solar Wind Streams. Geophysical Monograph Series, vol. 167. AGU, Washington, D.C, pp. 197–212.

Lu, G., 2006. High-speed streams, coronal mass ejections, and interplanetary shocks: a comparative study of geoeffectiveness. In: Tsurutani, B.T., McPherron, R.L., Gonzalez, W.D., Lu, G., Sobral, J.H.A., Gopalswamy, N. (Eds.), Recurrent Magnetic Storms: Corotating Solar Wind Streams. Geophysical Monograph Series, vol. 167. AGU, Washington, D.C, pp. 97–111.

McIntosh, D.H., 1959. On the annual variation of magnetic disturbance. Philos. Trans. R. Soc. Lond. Ser. A 251, 525–552.

McPherron, R.L., Weygand, J., 2006. The solar wind and geomagnetic activity as a function of time relative to corotating interaction regions. In: Tsurutani, B.T., McPherron, R.L., Gonzalez, W.D., Lu, G., Sobral, J.H.A., Gopalswamy, N. (Eds.), Recurrent Magnetic Storms: Corotating Solar Wind Streams. Geophysical Monograph Series, vol. 167. AGU, Washington, D.C, pp. 125–137.

Meredith, N.P., Cain, M., Horne, R.B., Thorne, R.M., Summers, D., Anderson, R.R., 2003. Evidence for chorus-driven electron acceleration to relativistic energies from a survey of geomagnetically disturbed periods. J. Geophys. Res. 108, 1248. http://dx.doi.org/10.1029/2002JA009764.

Murayama, T., 1974. Origin of the semiannual variation of geomagnetic Kp indices. J. Geophys. Res. 79, 297–300.

Mursula, K., Tanskanen, E., Love, J.J., 2011. Spring-fall asymmetry of substorm strength, geomagnetic activity and solar wind: implications for semiannual variation and solar hemispheric asymmetry. Geophys. Res. Lett. 38, L06104. http://dx.doi.org/10.1029/2011GL046751.

Paulikas, G., Blake, J.B., 1979. Effects of the solar wind on magnetospheric dynamics: Energetic electrons at the synchronous orbit. In: Olsen, W. (Ed.), Quantitative Modeling of Magnetospheric Processes. Geophysical Monograph Series, vol. 21. AGU, Washington, D.C, p. 21.

Pizzo, V.J., 1985. Interplanetary shocks on the large scale: a retrospective on the last decade's theoretical efforts. In: Tsurutani, B.T., Stone, R.G. (Eds.), Collisionless Shocks in the Heliosphere: Reviews of Current Research. Geophysical Monograph Series, vol. 35. AGU, Washington, D.C, pp. 51–68.

Priester, W., Catanni, D., 1962. On the semiannual variation of geomagnetic activity and its relation to the solar corpuscular radiation. J. Atmos. Sci. 19, 121–126.

Richardson, I.G., Cane, H.V., Cliver, E.W., 2002. Sources of geomagnetic activity during nearly three solar cycles (1972–2000). J. Geophys. Res. 107, A81187. http://dx.doi.org/10.1029/2001JA000504.

Riley, P., Linker, J.A., Mikić, Z., 2002. Modeling the heliospheric current sheet: solar-cycle variations. J. Geophys. Res. 107, http://dx.doi.org/10.1029/2001JA000299.

Rostoker, G., Falthammar, C., 1967. Relationship between changes in the interplanetary magnetic field and variations in the magnetic field at the Earth's surface. J. Geophys. Res. 72, 5853–5863.

Sabine, E., 1852. On periodical laws discoverable in the mean effects of the larger magnetic disturbances. No. II. Philos. Trans. R. Soc. Lond. 142, http://dx.doi.org/10.1098/rstl.1852.0009.

Smith, E.J., 2001. The heliospheric current sheet. J. Geophys. Res. 106, 15819–15831.

Smith, E.J., Wolfe, J.H., 1976. Observations of interaction regions and corotating shocks between one and five AU: pioneers 10 and 11. Geophys. Res. Lett. 3, 137–140. http://dx.doi.org/10.1029/GL003i003p00137.

Smith, E.J., Tsurutani, B.T., Rosenberg, R.L., 1978. Observations of the interplanetary sector structure up to helographic latitudes of 16°: pioneer 11. J. Geophys. Res. 83, 717–724.

Summers, D., Thorne, R.M., Xiao, F., 1998. Relativistic theory of wave-particle resonant diffusion with application to electron acceleration in the magnetosphere. J. Geophys. Res. 103, 20487–20500. http://dx.doi.org/10.1029/98JA01740.

Tsurutani, B.T., Gonzalez, W.D., 1987. The cause of high-intensity long-duration continuous AE activity (HILDCAAs): interplanetary Alfvén wave trains. Planet. Space Sci. 35, 405–412.

Tsurutani, B.T., Gonzalez, W.D., 1997. The interplanetary causes of magnetic storms: a review. In: Tsurutani, B.T., et al. (Eds.), Magnetic Storms. Geophysical Monograph Series, vol. 98. AGU, Washington, D.C, pp. 77–89.

Tsurutani, B.T., Gonzalez, W.D., Gonzalez, A.L.C., Tang, F., Arballo, J.K., Okada, M., 1995. Interplanetary origin of geomagnetic activity in the declining phase of the solar cycle. J. Geophys. Res. 100, 21717–21733. http://dx.doi.org/10.1029/95JA01476.

Tsurutani, B.T., Gonzalez, W.D., Guarnieri, F.L., Kamide, Y., Zhou, X., Arballo, J.K., 2004. Are high-intensity long-duration continuous AE activity (HILDCAA) events substorm expansion events? J. Atmos. Sol. Terr. Phys. 66, 167–176.

Tsurutani, B.T., Lakhina, G.S., Pickett, J.S., Guarnieri, F.L., Lin, N., Goldstein, B.E., 2005. Nonlinear Alfvén waves, discontinuities, proton perpendicular acceleration, and magnetic holes/decreases in interplanetary space and the magnetosphere: intermediate shocks? Nonlin. Proc. Geophys. 12, 321–336.

Tsurutani, B.T., Gonzalez, W.D., Gonzalez, A.L.C., Guarnieri, F.L., Gopalswamy, N., Grande, M., Kamide, Y., Kasahara, Y., Lu, G., McPherron, R.L., Soraas, F., Vasyliunas, V., 2006a. Corotating solar wind streams and recurrent geomagnetic activity: a review. J. Geophys. Res. 111, http://dx.doi.org/10.1029/2005JA011273 (A07S01).

Tsurutani, B.T., McPherron, R.L., Gonzalez, W.D., Lu, G., Gopalswamy, N., Guarnieri, F. L., 2006b. Magnetic storms caused by corotating solar wind streams. In:

Tsurutani, B., McPherron, R.L., Gonzalez, W.D., Lu, G., Sobral, J.H.A., Gopalswamy, N. (Eds.), Recurrent Magnetic Storms: Corotating Solar Wind Streams. Geophysical Monograph Series, vol. 167. AGU, Washington, D.C, pp. 1–17.

Tsurutani, B.T., Echer, E., Gonzalez, W.D., 2011a. The solar and interplanetary causes of the recent minimum in geomagnetic activity (MGA23): a combination of midlatitude small coronal holes, low IMF Bz variances, low solar wind speeds and low solar magnetic fields. Ann. Geophys. 29, 839–849.

Tsurutani, B.T., Echer, E., Guarnieri, F.L., Gonzalez, W.D., 2011b. The properties of two solar wind high speed streams and related geomagnetic activity during the declining phase of solar cycle 23. J. Atmos. Sol. Terr. Phys. 73, 164–177.

Turner, N.E., Mitchell, E.J., Knipp, D.J., Emery, B.A., 2006. Energetics of magnetic storms driven by corotating interaction region: a study of geoeffectiveness. In: Tsurutani, N., McPherron, R.L., Gonzalez, W.D., Lu, G., Sobral, J.H.A., Gopalswamy, N. (Eds.), Recurrent Magnetic Storms: Corotating Solar Wind Streams. Geophysical Monograph Series, vol. 167. AGU, Washington, D.C, pp. 113–124.

Wrenn, G.L., 1995. Conclusive evidence for internal dielectric charging anomalies on geosynchronous communications spacecraft. J. Spacecr. Rockets 32, 514–520. http://dx.doi.org/10.2514/3.26645.

Xanthakis, J., Poulakos, C., Petropoulos, B., 1988. Possible periodicities of high-speed solar plasma. Astrophys. Space Sci. 141, 233–250.